Avid Uptake of Technetium-99m-HMPAO by an Intracranial Plasmacytoma during Carotid Balloon Test Occlusion

Mordechai Lorberboym, David Segal, Josef Machac, Chandranath Sen and Michael Sacher

Division of Nuclear Medicine, Department of Radiology and Departments of Neurosurgery and Diagnostic Radiology, Mount Sinai School of Medicine, New York, New York

A 56-yr-old woman was evaluated for removal of a tumor at the base of the skull. A test to determine the risk of carotid artery sacrifice was performed prior to surgery using carotid balloon occlusion of the left internal carotid artery and ^{99m}Tc-HMPAO perfusion scintigraphy during the occlusion. An unusual intense focus of increased uptake was seen at the site of the primary tumor in the left cavernous sinus. The tumor, found to be plasmacytoma at surgery, demonstrated only mild washout from 30 min to 2 hr after administration of ^{99m}Tc-HMPAO, with a tumor-to-cerebellum ratio of 1.6 and 1.5, respectively, and a tumor-to-contralateral cranial ratio of 2.5 and 2.4, respectively. Intracranial plasmacytoma shows good response to radiation therapy, and the differentiation of this tumor from other neoplasms is pertinent to the mode of treatment and surgical approach. Technetium-99m-HMPAO SPECT imaging may be a useful tool in distinguishing these tumors from other neoplasms at the base of the skull.

Key Words: technetium-99m-HMPAO; carotid artery; occlusion; intracranial plasmacytoma; single-photon emission computed tomography

J Nucl Med 1995; 36:800–803

A cerebral blood flow study using ^{99m}Tc-HMPAO and SPECT imaging is a readily available, accurate technique for detecting perfusion abnormalities in patients with aneurysms and various tumors of the head and neck during balloon test occlusion (*1*). Patients at high risk of developing neurological deficits following permanent carotid occlusion may require a different surgical technique (*2*). Surgical approaches also may change depending on the tumor type because some tumors show an excellent response to radiation therapy and do not require complete excision. We report a case of intracranial plasmacytoma intracranial plasmacytoma at the base of the skull detected by ^{99m}Tc-HMPAO brain SPECT.

Received Aug. 8, 1994; revision accepted Nov. 7, 1994.

For correspondence or reprints contact: Mordechai Lorberboym, MD, Department of Nuclear Medicine, Mount Sinai Medical Center, One Gustave L. Levy Pl., New York, NY 10029.

CASE REPORT

A 56-yr-old woman presented with headache and diplopia. Physical examination was unremarkable, except for paralysis of the left sixth cranial nerve. Her blood count and blood chemistry tests were normal. CT revealed an enhancing mass in the left petrous apex extending into the posterior cavernous sinus and the sphenoid sinus (Fig. 1). A presumptive diagnosis of chordoma or chondrosarcoma was made. Prior to surgery, the patient underwent balloon test occlusion of the left internal carotid artery; she tolerated the procedure well without neurological deficit. The carotid angiogram at the time of the test occlusion showed a vascular tumor at the base of the skull (Fig. 2) and the differential diagnosis was expanded to include meningioma and hemangiopericytoma. Brain perfusion SPECT imaging was performed using a dual-head gamma camera equipped with a low-energy, high-resolution collimator. Imaging began 30 min following intravenous injection of 740 MBq ^{99m}Tc-HMPAO. Ninety-six 30-sec frames were acquired, and the images were prefiltered using a Butterworth filter (cutoff frequency = 0.2 cycles/cm; power factor = 5). One-pixel thick transaxial, coronal and sagittal slices were reconstructed and displayed on a 128 × 128 matrix. No attenuation correction was used.

SPECT images demonstrated a focus of intense activity at the base of the skull on the left in the region of the left cavernous sinus (Fig. 3). The patient underwent left fronto-temporal craniotomy and zygomatic osteotomy with cavernous sinus exploration. The tumor appeared to involve the left petrous bone and cavernous sinus. Partial tumor resection was performed and the frozen section was reported as plasmacytoma. Limited additional resection was performed and the surgery was completed. The final pathological report confirmed the diagnosis of plasmacytoma. Serum protein electrophoresis revealed low total protein of 6.1 g/dl (normal, 6.5–8.5 g/dl) with elevated alpha 1 globulin of 0.39 g/dl (normal, 0.1–0.3 g/dl) and a prominent band in the gamma region. Serum immunoelectrophoresis revealed increased IgA of 1350 mg/dl (normal, 100–400 mg/dl) with a monoclonal kappa spike and decreased IgM and IgG. Urine electrophoresis was normal. Radiographic bone survey showed multiple, small lucencies in the skull consistent with multiple myeloma. Bone marrow aspiration confirmed the diagnosis of multiple myeloma and the patient was referred for chemotherapy and radiation therapy 4 wk after surgery.

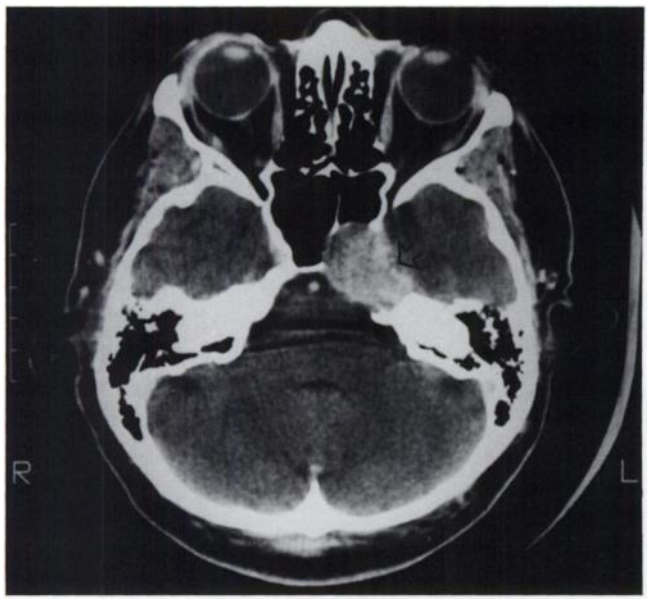

FIGURE 1. Contrast-enhanced transaxial CT scan demonstrates a homogeneously enhancing mass (arrow) with extension of the tumor into the sphenoid sinus and bony erosion of the petrous apex.

DISCUSSION

Multiple myeloma is a plasma cell neoplasm characterized by malignant proliferation of plasma cells, infiltration of bone marrow and monoclonal immunoglobulin synthesis. Two variants of plasma cell neoplasms are extramedullary plasmacytoma and solitary plasmacytoma of bone (*3–5*). There is a general consensus that extramedullary plasmacytoma constitutes a different disease process from solitary plasmacytoma of bone and myeloma and has a different natural history (*3*). Progression of solitary plasmacytoma of bone to multiple myeloma has been reported in 33%–75% of cases and progression of extramedullary plasmacytoma to multiple myeloma has been observed in 0%–33% (*5*). Solitary plasmacytoma of bone continues to convert to multiple myeloma even after 17 yr, which may suggest that these tumors are actually multiple myeloma in evolution (*6*). More than 75% of plasmacytomas occur in the head and neck region. The tumor may involve the base of the skull and lead to cranial nerve palsies, invade the orbit and produce a picture of orbital space-occupying lesions or extend intracranially (*7*). Lesions at the base of the skull are commonly located at the body of the sphenoid and the apex of the petrous bone, as occurred in our patient. Most tumors in this region probably originate from the bone, but it has been suggested that they may arise from mucosa contained within the sphenoid and petrous bones (*8*). Local control of the disease may be achieved in patients with incomplete resection following additional radiation and/or chemotherapy (*3–4*). Therefore, it is important to diagnose the disease as early as possible because a relatively high cure rate can be achieved. Unlike multiple myeloma, plasmacytomas are radiosensitive and there is a better prognosis. In Stage I disease (localized to the primary site), chemotherapy may be curative or at least may delay the time to conversion (*4,6*).

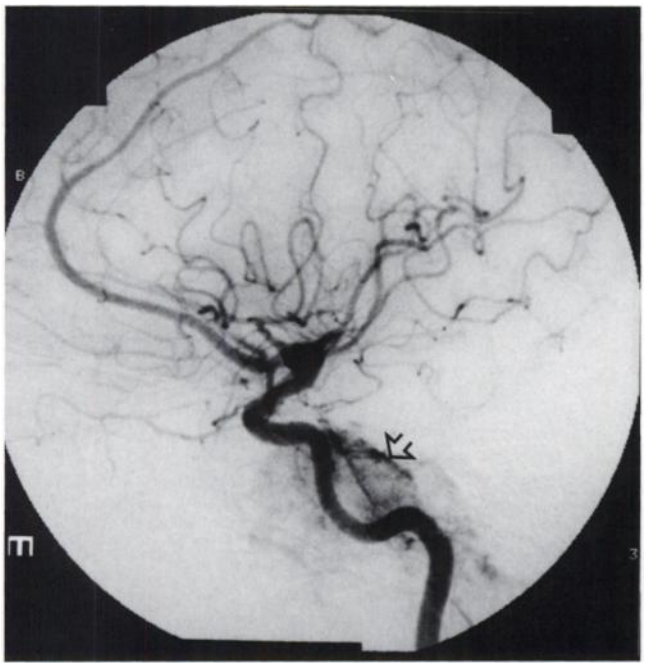

FIGURE 2. A left internal carotid angiogram demonstrates a tumor blush (arrow) with minimal encasement of the vertical portion of the internal carotid artery.

Many cases of multiple myeloma are accompanied by signs of increased intracranial pressure (*10,11*), but clinical or radiographic findings are not diagnostic. Age and sex distribution, clinical and roentgenographic findings may in fact mimic the features of meningiomas (*11*). Intracerebral plasmacytomas usually reveal a high attenuation mass on CT scans that enhance with contrast material administration and may be associated with brain edema and mass effect (*11,12*). Intratumoral hemorrhage may also occur (*13*). Magnetic resonance (MR) imaging may detect foci of disease not detected on conventional radiographs in patients with multiple myeloma. The MR appearance, however, resembles that of other primary or secondary malignancies that produce lytic destruction of bone (*14*).

Technetium-99m-HMPAO is a lypophilic amine which shows rapid brain uptake and distributes proportionally to regional blood flow (*17,18*). The tracer is converted intracellularly to a hydrophilic compound in the presence of glutathione (*19*) and remains fixed in the brain for a prolonged time. Various types of brain tumors were evaluated with ^{99m}Tc-HMPAO, mainly gliomas and meningiomas (*20*). Langen et al. (*21*) found no significant difference in the uptake of ^{99m}Tc-HMPAO among primary malignant gliomas, recurrent malignant gliomas or low-grade gliomas. Meningiomas, however, exhibited significantly higher ^{99m}Tc-HMPAO uptake (with the highest tumor-to-cerebellum ratio of 1.14 ± 0.31). Delayed scans showed considerable decrease in tumor uptake after 2 hr and it was postulated that the damaged blood-brain barrier in the tumor allowed the trapped hydrophilic component of ^{99m}Tc-

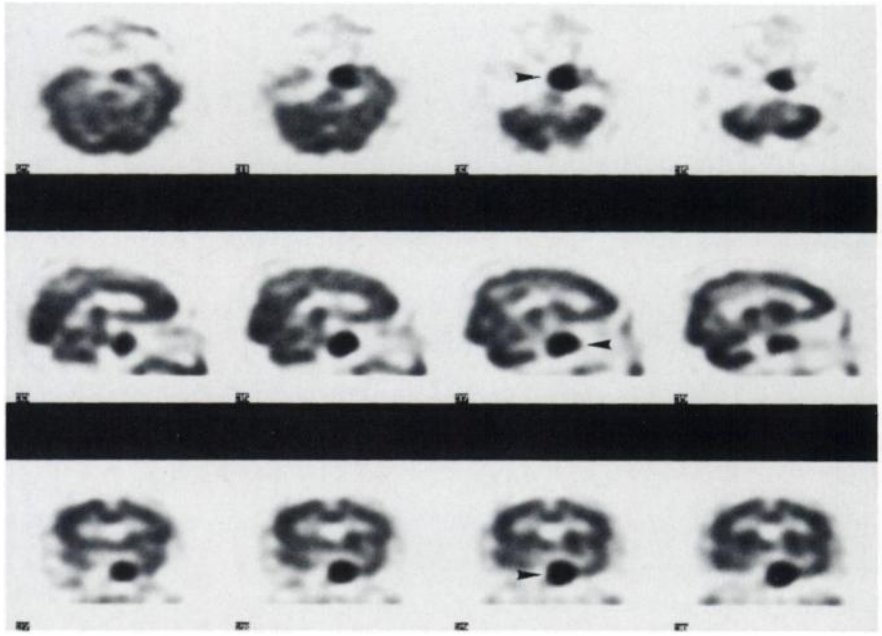

FIGURE 3. Axial, sagittal and coronal images (upper, middle and lower row, respectively) of ^{99m}Tc-HMPAO brain SPECT shows intensely increased activity (arrows) at the base of the skull.

HMPAO complex to leave the tissue. In contrast, Ohnishi et al. (*22*) noticed that ^{99m}Tc-HMPAO distribution in benign and malignant thyroid tumors was independent of time from 2 to 120 min after injection; this is similar to the findings in our patient.

Uptake of ^{99m}Tc-HMPAO in metastatic lesions may be related to tumor neovascularity and facilitated transport across abnormal vessel walls and cell membranes (*23*). Although tumor cell kinetics of the tracer is unknown, it is apparent that tumor uptake is not only a function of regional cerebral blood flow and blood-brain barrier permeability but also a function of the affinity of certain tumor types to ^{99m}Tc-HMPAO and the presence of arteriovenous shunting, necrosis and edema (*24*). The plasmacytoma in our patient showed an outstanding tumor-to-cerebellum and tumor-to-background ratio (considering the high background activity from ^{99m}Tc-HMPAO) with persistent retention of activity in the tumor for 2 hr. This avid uptake, more prominent than the uptake previously reported in meningiomas (*21*), is explained in part by the high vascularity and metabolic activity of the tumor, but also by the absence of damaged blood-brain barrier (due to the extracerebral location of the tumor) which allows leakage of the hydrophilic component of ^{99m}Tc-HMPAO from the cells. Further investigation is necessary to determine if this tumor type can be differentiated from other neoplasms at the base of the skull because it may significantly affect the treatment modality and surgical approach.

The small lesions in the skull noted on the radiographic bone survey were not observed on the ^{99m}Tc-HMPAO scan, even when using high contrast images. This is attributed to smaller lesion size but may also signify a different tumor physiology.

CONCLUSION

Although CT and MRI can delineate the anatomy and location of intracranial tumors, the correlation of these imaging modalities and angiography with perfusion SPECT imaging may better characterize the pathophysiology of some brain tumors, such as plasmacytoma, and possibly increase the specificity of the study.

ACKNOWLEDGMENT

The authors thank Ms. Veronica Cody for her excellent administrative work.

REFERENCES

1. Palestro CJ, Sen C, Muzinic M, Afriyie M, Goldsmith SJ. Assessing collateral cerebral perfusion with technetium-99m-HMPAO SPECT during temporary internal carotid artery occlusion. *J Nucl Med* 1993;34:1235–1238.
2. Mathews D, Walker BS, Purdy PD, et al. Brain blood flow SPECT in temporary balloon occlusion of carotid and intracerebral arteries. *J Nucl Med* 1993;34:1239–1243.
3. Gaffney CC, Dawes PJ, Jackson D. Plasmacytoma of the head and neck. *Clin Radiol* 1987;38:385–388.
4. Soesan M, Paccagnella A, Chiarion-Sileni V, et al. Extramedullary plasmacytoma: clinical behavior and response to treatment. *Ann Oncol* 1992;3:51–57.
5. Greenberg P, Parker RG, Fu YS, Abemayor E. The treatment of solitary plasmacytoma of bone and extramedullary plasmacytoma. *Am J Clin Oncol* 1987;10:199–204.
6. Holland J, Trenkner DA, Wasserman TH, Fineberg B. Plasmacytoma. *Cancer* 1992;69:1513–1517.
7. Clarke E. Cranial and intracranial myelomas. *Brain* 1954;77:61–81.
8. Cappell DF, Mathers RP. Plasmacytoma of petrous temporal bone and base of skull. *J Laryng Otol* 1935;50:340–349.
9. Penny R, Hughes S. Repeated stimulation of the reticuloendothelial system and the development of plasma-cell dyscrasias. *Lancet* 1970;1:77–78.
10. Plant GT, Donald JJ, Jackowski A, Vinnicombe SJ, Kendall BE. Partial, nonthrombotic, superior sagittal sinus occlusion due to occipital skull tumours. *J Neurol Neurosurg Psych* 1991;54:520–523.
11. Atweh GF, Jabbour N. Intracranial solitary extraskeletal plasmacytoma resembling meningioma. *Arch Neurol* 1982;39:57–59.

12. Wisniewski T, Sisti M, Inhirami G, Knowles DM, Powers JM. Intracerebral solitary plasmacytoma. *Neurosurgery* 1990;27:826–829.
13. Husain MM, Metzer WS, Binet EF. Multiple intraparenchymal brain plasmacytomas with spontaneous intratumoral hemorrhage. *Neurosurgery* 1987;20:619–623.
14. Moulopoulos LA, Dimopoulos MA, Weber D, Fuller L, Libshitz HI, Alexanian R. Magnetic resonance imaging in the staging of solitary plasmacytoma of bone. *J Clin Oncol* 1993;11:1311–1315.
15. Lucignani G, Rossetti C, Ferrario P, et al. In vivo metabolism and kinetics of ^{99m}Tc-HMPAO. *Eur J Nucl Med* 1990;16:249–255.
16. Holman BL, Devous MD Sr. Functional brain SPECT: the emergence of a powerful clinical method. *J Nucl Med* 1992;33:1888–1904.
17. Andersen AR, Fribert H, Knudsen KBM et al. Extraction of [^{99m}Tc]-d, 1-HM-PAO across the blood-brain barrier. *J Cereb Blood Flow Metab* 1988;8:S44–S51.
18. Neirinckx RD, Canning LR, Piper IM, et al. Technetium-99m-d, 1-HM-PAO: a new radiopharmaceutical for SPECT imaging of regional cerebral blood perfusion. *J Nucl Med* 1987;28:191–202.
19. Neirinckx RD, Burke JF, Harrison RC, Forster AM, Andersen AR, Lassen NA. The retention mechanism of ^{99m}Tc HMPAO: intracellular reaction with glutathione. *J Cereb Blood Flow Metab* 1988;8:S4–S12.
20. Biersack HJ, Grunwald F, Kropp J. Single photon emission computed tomography imaging of brain tumors. *Semin Nucl Med* 1991;21:2–10.
21. Langen KJ, Roosen N, Herzog H, et al. Investigations of brain tumours with ^{99m}Tc-HMPAO SPECT. *Nucl Med Commun* 1989;10:325–334.
22. Ohnishi T, Noguchi S, Murakami N, et al. Early and delayed imaging of ^{99m}Tc-HMPAO versus ^{201}Tl in benign and malignant thyroid tumors. Similar uptake but different retention. *Clin Nucl Med* 1992;17:806–811.
23. Sole-Llenas J, Mercader JM, Pons-Tortella E. Morphological aspects of the vessels of brain tumors. *Neuroradiology* 1977;13:51–54.
24. Lindegaard MW, Skretting A, Hager B, et al. Cerebral and cerebellar uptake of ^{99m}Tc-(d,l)hexamethyl-propylene-amine oxime (HM-PAO) in patients with brain tumors studied by single photon emission computerized tomography. *Eur J Nucl Med* 1986;12:417–420.